Synthesis and Structure of Bis(π-cyclopentadienyl)vanadium(IV) 1,10-Phenanthroline and 2,2′-Bipyridine Compounds and Their Interactions with Artificial Membranes

Phalguni Ghosh,[†] Ann T. Kotchevar,[†] Darin D. DuMez,[†] Sutapa Ghosh,[‡] John Peiterson,[†] and Fatih M. Uckun*[,§]

Departments of Chemistry and Structural Biology, and Drug Discovery Program, Hughes Institute, St. Paul, Minnesota 55113

Received February 26, 1999

The reaction of in situ generated $Cp_2V(OTf)_2$ (Cp = cyclopentadienyl; OTf = O_3SCF_3) with excess 1,10-phenanthroline and 2,2′-bipyridine yields the d^1 vanadocene coordination compounds $[Cp_2V(phen)][OTf]_2$ (**1**) and $[Cp_2V(bpy)][OTf]_2$ (**2**), respectively. The compounds have been characterized by UV−vis and EPR spectroscopy and by cyclic voltammetry. The complexes have relatively low vanadium(IV)−vanadium(III) reduction potentials (−0.62 V vs $Cp_2Fe^{+/0}$ in acetonitrile). Structures of **1** and **2** have been determined by X-ray crystallography. Compound **1** crystallized in a monoclinic system, space group $P2_1/n$, with $a = 10.2763(5)$ Å, $b = 18.1646(9)$ Å, $c = 13.5741(7)$ Å, $\beta = 99.4150(10)°$, and $Z = 4$. Refinement of its structure by full-matrix least-squares techniques gave final residuals $R = 0.040$ and $R_w = 0.096$. Compound **2** crystallized in a monoclinic system, space group $P2_1/c$, with $a = 10.6451(6)$ Å, $b = 18.3863(10)$ Å, $c = 12.6993(7)$ Å, $\beta = 98.6220(10)°$, and $Z = 4$. Refinement of its structure by full-matrix least-squares techniques gave final residuals $R = 0.046$ and $R_w = 0.101$. The two nitrogen atoms and centroids of the two cyclopentadienyl rings for both compounds occupy a distorted tetrahedral geometry around the vanadium(IV) center. The chelated ring plane is inclined closer to one of the neighboring Cp rings with the tilt more evident in **1** (∼8°) than **2** (∼4°). The membrane interactions of these compounds and the titanium analogues, $[Cp_2Ti(phen)][OTf]_2$ (**3**) and $[Cp_2Ti(bpy)][OTf]_2$ (**4**), have been studied with zwitterionic unilamellar liposomes as artificial membranes. We show that the ability of metallocenes to enhance the permeability of a liposomal membrane depends on the hydrophobicity, as well as the size and planarity of the ancillary chelated ligands, but not the nature of the central metal ion. Also provided is evidence that metallocene-induced permeability changes in artificial membranes are not caused by lipid peroxidation.

Introduction

Investigations into the coordination chemistry of vanadocene(IV) L_2 (L is a monodentate ligand) or vanadocene(IV) (L-L) (L-L is a bidentate ligand) complexes have been for the most part to delineate the electronic structures and bonding properties of these d^1 systems.[1−10] Their potential applications as catalysts, especially the use of vanadocene dihalides in olefin polymerization reactions, have been the subject of interest for the past several decades.[11,12] There has also been a growing interest in examining the biological effects[13−15] of vanadocene complexes and studying their chemistry under physiological conditions.[16−19] Recently, interest in the synthesis and characterization of new vanadocene(IV) complexes has grown due to the demonstration of their spermicidal activity and apoptosis-inducing properties.[20−23] These spermicidal vanadocene complexes caused depolarization in the mitocondrial membrane without disrupting the human sperm membranes.[20,21] These results encouraged us to synthesize new vanadocene(IV) complexes and examine their surface interactions with artificial membranes.

Studies of the physical interactions of metal complexes with model membrane systems have also been the subject of recent

* Corresponding author. Phone: (651) 697-9228. Fax: (612) 697-1042. E-mail: fatih_uckun@mercury.ih.org.
[†] Department of Chemistry.
[‡] Department of Structural Biology.
[§] Drug Discovery Program.

(1) Stewart, C. P.; Porte, A. L. *J. Chem Soc., Dalton. Trans.* **1973**, 722.
(2) Casey, A. T.; Thackeray, J. R. *Aust. J. Chem.* **1972**, *25*, 2085.
(3) Casey, A. T.; Thackeray, J. R. *Aust. J. Chem.* **1974**, *27*, 757.
(4) Petersen, J. L.; Dahl, L. F. *J. Am. Chem. Soc.* **1975**, *97*, 6422.
(5) Petersen, J. L.; Lichtenberger, D. L.; Fenske, R. F.; Dahl, L. F. *J. Am. Chem. Soc*. **1975**, *97*, 6433.
(6) Lauher, J. W.; Hoffmann, R. *J. Am. Chem. Soc*. **1976**, *98*, 1729.
(7) Muller, E. G.; Watkins, S. F.; Dahl, L. F. *J. Organomet. Chem.* **1976**, *111*, 91.
(8) Gambarotta, S.; Floriani, C.; Chiesi-Villa, A.; Guastini, C. *Inorg. Chem.* **1984**, *23*, 1739.
(9) Stephan, D. *Inorg. Chem*. **1992**, *31*, 4218.
(10) Tzavellas, N.; Klouras, N.; Raptopoulou, C. P. *Z. Anorg. Allg. Chem.* **1996**, *622*, 898.
(11) Hercules Powder Co. U.S. Patent 2 924 594, 1960 (*Chem. Abstr*. **1960**, *54*, 11573).
(12) Karapinka, G. L.; Carrick, W. L. *J. Polym. Sci*. **1961**, *55*, 145.
(13) Köpf-Maier, P.; Köpf, H. *Z. Naturforsch.* **1979**, *34B*, 805.
(14) Köpf-Maier, P.; Köpf, H. *Struct. Bonding* (*Berlin*) **1988**, *70*, 103 and references therein.
(15) Toney, J. H.; Rao, L. N.; Murthy, M. S.; Marks, T. J. *Breast Cancer Res. Treat.* **1985**, *6*, 185.
(16) Toney, J. H.; Marks, T. J. *J. Am. Chem. Soc*. **1985**, *107*, 947.
(17) Toney, J. H.; Brock, C. P.; Marks, T. J. *J. Am. Chem. Soc*. **1986**, *108*, 7263.
(18) Kuo, L. Y.; Kanatzidis, M.; Sabat, M.; Tipton, A. L.; Marks, T. J. *J. Am. Chem. Soc*. **1991**, *113*, 9027.
(19) Toney, J. H.; Rao, L. N.; Murthy, M. S.; Marks, T. J. *Chem.-Biol. Interact.* **1985**, *56*, 45.
(20) D'Cruz, O. J.; Ghosh, P.; Uckun, F. M. *Biol. Reprod*. **1998**, *58*, 1515.
(21) D'Cruz, O. J.; Ghosh, P.; Uckun, F. M. *Mol. Hum. Reprod*. **1998**, *4*, 683.
(22) Ghosh, P.; Ghosh, S.; D'Cruz, O. J.; Uckun, F. M. *J. Inorg. Biochem*. **1998**, *72*, 89.
(23) Aubrecht, J.; Narla, R. K.; Ghosh, P.; Staneck, J.; Uckun, F. M. *Toxicol. Appl. Pharm.* **1999**, *154*, 228.

10.1021/ic9902469 CCC: $18.00
Published on Web 07/23/1999

research activities.[24−27] In a micellar system, cationic octahedral Ru(II), Rh(III), and Co(III) coordination complexes with 2,2′-bipyridine, 1,10-phenanthroline, and 9,10-phenanthrequinone-diimine-type planar fused ring systems as ligands have been shown to bind in the Stern layer with the ligands inserted into the hydrophobic portion of the micelle.[24] A comparison of the equilibrium constants for the association of cationic complexes with anionic micelles revealed that hydrophobic effects dominate the binding properties.[28,29] Hydrophobic ligands, in fact, have been shown to be able to overcome electrostatic repulsions and cause positively charged coordination compounds to bind to like-charged micelles.[30−33]

Previously, metal complex−liposome interaction studies were limited to inorganic salts in which the ability of the species to cause lipid peroxidation was considered essential to its ability to alter the physical properties of the liposomal membrane.[34−37] In our earlier report, experimental evidence suggested that some vanadocene-chelated complexes cause changes in the permeability of liposomal membranes.[38] Those vanadocene complexes caused the release of an encapsulated dye from both zwitterionic and anionic liposomes. This ability was not related to the extent of peroxidation of the lipids or to the complete disruption of the membrane. We proposed that these vanadocene-chelated complexes altered the membrane by intercalation, creating leaky patches in the liposomal membrane.

In this paper, we detail the characterization and the crystal structures of two new complexes, $[Cp_2V(phen)][OTf]_2$ (**1**) and $[Cp_2V(bpy)][OTf]_2$ (**2**) (Cp = cyclopentadienyl; OTf = O_3SCF_3). As a further extension of model membrane−complex

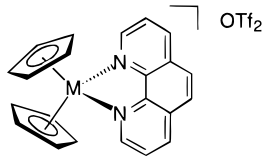

M = V (**1**), Ti (**3**)

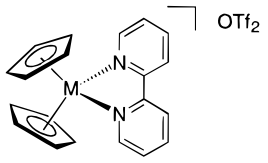

M = V (**2**), Ti (**4**)

interaction studies, we have also compared these two compounds to their titanium analogues (**3**, **4**) in order to determine the importance of the ancillary chelated ligands versus the metal center for the membrane-permeabilizing action of metallocene complexes. The effects of the complexes on lipid peroxidation are also compared.

Experimental Section

Abbreviations. Cp = cyclopentadienyl; bpy = 2,2′ bipyridine; phen = phenanthroline; OTf = O_3SCF_3; PBS = phosphate buffered saline; THF = tetrahydrofuran; POBN = α-(4-pyridyl-1-oxide)-*N*-*tert*-butylnitrone; PC = phosphatidylcholine.

General Procedures. Syntheses were performed under an inert atmosphere using standard Schlenk techniques, unless otherwise noted. $[Cp_2Ti(phen)][OTf]_2$ (**3**) and $[Cp_2Ti(bpy)][OTf]_2$ (**4**) were prepared according to literature procedures.[39] Egg yolk phosphatidylcholine was purchased from Avanti Polar Lipids (Alabaster, AL). 5(6)-Carboxyfluorescein was from Molecular Probes, Inc. (Eugene, OR). All other reagents were purchased from Aldrich Chemical Co. (Milwaukee, WI) and used without modification unless stated otherwise. Acetonitrile and methylene chloride were dried over CaH_2 and distilled prior to use. THF was dried over sodium and distilled prior to use.

Infrared spectra were obtained on a FT-Nicollet Protege 460 spectrometer as KBr pellets or Nujol mulls. IR spectra are reported in cm^{-1}. UV−vis spectra were recorded in a quartz cell or cuvette on a Beckman model DU 7400 spectrophotometer, and the spectral bands were registered in the 250−800 nm range. ^1H NMR spectra were recorded on a Varian XL-300 spectrometer operating at 300.110 MHz. Chemical shifts were referenced to residual protio solvent peaks in the sample. Magnetic moments were determined using Evans' Method at 20 °C.[40] Mass spectra were recorded on a HP G2025A MALDI-TOF mass spectrometer using α-cyano-4-hydroxycinnamic acid as the supporting matrix. Spectra were averaged over 50 shots. Electron paramagnetic resonance (EPR) spectra were recorded in PBS (0.015 M $NaHPO_4$, 0.10 M NaCl, 0.02 M KCl, pH 7.2) or acetonitrile on a Bruker ESP 300 EPR spectrometer (9.64 GHz). The *g* values were calibrated with a Varian strong pitch (0.1% in KCl) standard (*g* value of 2.0028). The samples for the EPR spectral analysis were studied in a Willmad WG-814 standard TE102 aqueous cell cavity (0.3-mm inner path length) to minimize the dielectric loss. All fluorescence measurements were made using a Shimadzu spectrofluorophotometer (model RF-5301PC). Electrochemical measurements were performed on a Bioanalytical Systems B/W 100b electrochemical analyzer with IR compensation. The cyclic voltammograms taken in acetonitrile were obtained in a 0.1 M Bu_4NPF_6 (TABP) electrolyte solution with a 0.1 M $Ag/AgNO_3$ reference electrode, a platinum disk working electrode, and a platinum wire auxiliary electrode. Solutions were purged with nitrogen and scanned at 200 mV/s. Aqueous cyclic voltammograms were taken in a standard PBS solution, using a Ag/AgCl reference electrode, a glassy carbon working electrode, and a platinum wire auxiliary electrode. Solutions were purged with nitrogen and scanned at 200 mV/s. All potentials were referenced to the ferrocene−ferrocenium couple. Elemental analyses were performed by Atlantic Microlab, Inc. (Norcross, GA).

$[Cp_2V(phen)][OTf]_2$ (1). The synthesis was based on a modification of the synthetic procedure reported by Thewalt et al. for $[Cp_2Ti(phen)][OTf]_2$.[39] Cp_2VCl_2 (253 mg, 1.0 mmol) and AgOTf (521 mg, 2.1 mmol) were placed in a 25 mL round-bottomed flask. THF (20 mL) was added, and the solution was stirred for 1.5 h. The solution was quickly filtered in air through Celite, and the filtrate was placed again under argon. A methylene chloride solution (15 mL) of 1,10-phenanthroline (271 mg, 1.5 mmol, 1.5 equiv) was added to the stirring solution, causing an immediate color change from green to muddy brown. The solution was stirred vigorously for 13 h, opened to the air, and then filtered. The gummy brown residue was washed with THF and hexanes. The resultant brown powder was then washed with acetone (3 × 5 mL), yielding a fine brown powder. The powder was recrystallized from a minimum of acetonitrile layered with ether. A 224 mg amount of **1** was obtained as large dark brown crystals (34% yield; 0.34 mmol). IR: 3134 (w), 3101 (m), 2951 (m), 1630 (w), 1606 (m), 1587 (m), 1448 (w), 1271 (s), 1260 (s), 1215 (m), 1152 (s), 1030 (s), 872 (w), 854 (m), 724 (m),

(24) Hackett, J. W.; Turro, C. *Inorg. Chem*. **1998**, *37*, 2039.
(25) Arkin, M. R.; Stemp, E. D. A.; Turro, C.; Turro, N. J.; Barton, J. K. *J. Am. Chem. Soc*. **1996**, *118*, 2269.
(26) Ottaviani, M. F.; Ghatlia, N. D.; Turro, N. J. *J. Phys. Chem*. **1992**, *96*, 6075.
(27) Kunjappu, J. T.; Somasundaran, P.; Turro, N. J. *J. Phys. Chem*. **1990**, *94*, 8464.
(28) Davies, K. M.; Hussam, A.; Rector, B. R.; Owen, I. M.; King, P. *Inorg. Chem*. **1994**, *33*, 1741.
(29) Davies, K. M.; Hussam, A. *Langmuir* **1993**, *9*, 3270.
(30) Jain, A.; Xu, W.; Demas, J. N.; DeGraff, B. A. *Inorg. Chem*. **1998**, *37*, 1876.
(31) Snyder, S. M.; Buell, S. L.; Demas, J. N.; DeGraff, B. A. *J. Phys. Chem*. **1989**, *93*, 5265.
(32) Dressick, W. J.; Hauenstein, B. L.; Demas, J. N.; DeGraff, B. A. *Inorg. Chem*. **1984**, *23*, 1107.
(33) Hauenstein, B. L.; Dressick, W. J.; Buell, S. L.; Demas, J. N.; DeGraff, B. A. *J. Am. Chem. Soc*. **1983**, *105*, 4251.
(34) Verstraeten, S. V.; Nogueira, L. V.; Schreier, S.; Oteiza, P. I. *Arch. Biochem. Biophys*. **1997**, *338*, 121.
(35) Verstraeten, S. V.; Oteiza, P. I. *Arch. Biochem. Biophys*. **1995**, *322*, 284.
(36) Zhang, D.; Yasuda, T.; Yu, Y.; Okada, S. *Acta Med. Okayama* **1994**, *48*, 131.
(37) Ohsumi, Y.; Kitamoto, K.; Anraku, Y. *J. Bacteriol*. **1988**, *170*, 2676.
(38) Kotchevar, A. T.; Ghosh, P.; Uckun, F. M. *J. Phys. Chem. B* **1998**, *102*, 10925.
(39) Thewalt, U.; Berhalter, K. *J. Organomet. Chem*. **1986**, *302*, 193.
(40) Evans, D. F. *J. Chem. Soc.* **1959**, 2003.

637 (s), 572 (w), 517 (m). UV−vis (CH_3CN, nm (ϵ)): 558 (92), 448 (sh), 355 (sh), 270 (29 300), 229 (38 800). $\mu_{eff}(CDCl_3) = 1.68(12)\ \mu_B$. MALDI-TOF MS: $m/z = 361$ (m − 2OTf$^+$). Anal. Calcd for $C_{24}H_{18}F_6N_2O_6S_2V$: C, 43.72; H, 2.75; N, 4.25. Found: C, 43.93; H, 2.87; N, 4.08.

[Cp$_2$V(bpy)][OTf]$_2$ (2). The synthesis was based on a modification of the synthetic procedure reported by Thewalt et al. for [Cp$_2$Ti(bpy)][OTf]$_2$.[39] Cp$_2$VCl$_2$ (252 mg, 1.0 mmol) and AgOTf (523 mg, 2.1 mmol) were placed in a 25 mL round-bottomed flask. THF (20 mL) was added, and the solution was stirred for 1.5 h. The solution was quickly filtered in air through Celite, and the filtrate was placed again under argon. A methylene chloride solution (15 mL) of 2,2′-bipyridine (325 mg, 2.08 mmol, 2.08 equiv) was slowly added to the solution, causing an immediate color change from deep green to a dark brown. The solution was stirred for a few minutes and allowed to stand for 14 h. The flask was opened to the air, and the solution was then filtered. The fine brown precipitate was washed with excess THF (40 mL) and hexanes (2 × 10 mL). The resultant brown powder was then washed with acetone three times, giving a fine brown powder. The powder was recrystallized from a minimum of acetonitrile layered with hexanes. A 267 mg amount of small reddish brown crystals of **2** was recovered (42% yield; 0.42 mmol). IR: 3121 (w), 3099 (m), 2951 (m), 1604 (m), 1474 (m), 1450 (w), 1437 (m), 1404 (m), 1285 (w), 1266 (vs), 1257 (s), 1225 (m), 1156 (s), 1028 (s), 864 (m), 772 (m), 637 (s), 573 (w), 516 (m). UV−vis (CH_3CN, nm (ϵ)): 598 (sh, 16 722), 556 (120), 444 (22 522), 319 (9 900), 242 (25 800). $\mu_{eff}(CDCl_3) = 1.66(12)\ \mu_B$. MALDI-TOF MS: $m/z = 337$ (m − 2OTf$^+$). Anal. Calcd for $C_{22}H_{18}F_6N_2O_6S_2V$: C, 41.59; H, 2.90; N, 4.41. Found: C, 41.81; H, 2.98; N, 4.36.

Crystallographic Structure Determinations of [Cp$_2$V(phen)][OTf]$_2$ (1) and [Cp$_2$V(bpy)][OTf]$_2$ (2). Rectangular shaped crystals of **1** were grown by vapor diffusion of hexane into an acetone solution of **1** at room temperature. A single crystal of dimensions 0.5 × 0.3 × 0.1 mm was attached to a glass fiber using epoxy and was used for cell constant determination and data collection. Dark green, prism shaped crystals of **2** were grown by vapor diffusion of hexane into an acetonitrile solution of **2** at room temperature. A single crystal of dimensions 0.4 × 0.2 × 0.2 mm was attached to a glass fiber using epoxy and was used for cell constant determination and data collection. Data were collected using a Bruker SMART platform CCD, with graphite monochromatic Mo $K\alpha$ radiation ($\lambda = 0.710\ 73$ Å) at room temperature (293 K). The SMART software[41] was used for data collection, and the SAINT program[42] was used for data reduction. An empirical absorption correction[43] was applied, and the structure was solved by direct methods using the SHELXTL V5.10 suite of programs.[43] All non-hydrogen atoms were refined anisotropically, and the hydrogen atoms were placed in ideal positions and refined as riding atoms with individual isotropic thermal parameters. Atomic scattering factors were taken from ref 44. All calculations were performed on a Pentium computer. Crystallographic data are summarized in Table 2. Selected bond lengths and angles are presented in Table 3, and ORTEP drawings are shown in Figures 4 and 5.

Carboxyfluorescein Leakage Experiments. Liposomes with 3:1 PC:cholesterol were formed in 0.1 M phosphate buffer, pH 7.2, using the ethanol injection method to a 1 mM total lipid concentration with carboxyfluorescein encapsulated under self-quenching conditions (0.1 M carboxyfluorescein). The liposomes encapsulated with carboxyfluorescein were separated from free carboxyfluorescein by passage over a Sephadex 25 column (Pharmacia Biotech) to give a final lipid concentration of 0.7 mM. Compounds **1** and **2** were dissolved in methanol, and the resultant solutions were added to the liposome solutions to final metal complex concentrations of 50−400 μM. Compounds **3** and **4** were less stable in methanol over long periods of time and so were dissolved in acetonitrile. These solutions were added to the liposome solutions in the same fashion.[45] The increase in fluorescence was monitored at $\lambda_{exc} = 490$ nm and $\lambda_{em} = 550$ nm for 6 min at 20 °C.[35,46] Complete liposome disruption was achieved by the addition of excess Triton X-100 (10 μL of a 10% aqueous solution). Carboxyfluorescein release was calculated as shown in eq 1 where CF

$$\text{CF}\ (\%) = [(F - F_0)/(F_t - F_0)] \times 100 \qquad (1)$$

= carboxyfluorescein release, F_0 = fluorescence intensity of the intact liposome, F = fluorescence intensity at time = 6 min, and F_t = fluorescence intensity with Triton X.

Lipid Peroxidation. Aliquots of 0.5 mL of liposomes (0.7 mM total lipid) were incubated with the metal complexes (50−400 μM) at 37 °C for 90 min. The incubation was stopped by the addition of 0.1 mL of 4% butylated hydroxytoluene in EtOH. Sodium dodecyl sulfate (3%, 0.25 mL) was added to destroy the liposomes followed by the addition of 0.5 mL of 1% 2-thiobarbituric acid in 0.05 M NaOH and 0.5 mL of 25% HCl. The samples were mixed and heated in boiling water for 15 min. The 2-thiobarbituric acid reactive substances were extracted into 3 mL of 1-butanol, and the fluorescence of the butanol layer was measured at $\lambda_{exc} = 515$ nm and $\lambda_{em} = 555$ nm.[34,35,47−49] The 2-thiobarbituric acid reactive substances are reported as malonaldehyde equivalents.[50]

Liposome Aggregation. The metal complexes were added to 0.5 mL portions of the liposome solutions (0.7 mM total lipid) to yield final concentrations of 50−400 μM vanadium or titanium. The aggregation of liposomes was measured as the increase in absorbance at 300 nm in a UV−vis spectrophotometer over 15 min at 20 °C.[35]

EPR Spin-Trapping Experiments. The following is a general procedure for the spin-trapping experiments: A 1×10^{-3} M solution of the vanadocene compound was prepared in water. POBN (5 equiv) was added to the solution, followed by the addition of excess H_2O_2 (10 equiv). The solution was transferred to a 50 μL capillary tube, which was mounted in the cavity of the EPR spectrometer, and the spectrum was taken. The spectra were taken within 90 s of the addition of H_2O_2 unless otherwise noted, and each spectrum was averaged from four independent scans. The EPR spectra of the POBN −$^\bullet$OH adducts were identified by their doublet of triplet EPR signals of the hydroxyl radical at $g = 2.008$ with hyperfine splitting of the nitrosyl nitrogen, $\langle A^N \rangle = 15 \times 10^{-4}$ cm^{-1}, and the β-hydrogen atom, $\langle A^H \rangle = 2.81 \times 10^{-4}$ cm^{-1}, using $VOSO_4$ as a standard.[51] Control solutions of the organometallic vanadium compounds and POBN indicated no interaction between the compounds and the spin trap. Control solutions of POBN and H_2O_2 also indicated no interaction between just the spin trap and H_2O_2.

Results and Discussion

Synthesis. Reaction of in situ generated Cp$_2$V(OTf)$_2$ in dry THF with 2,2′-bipyridine and 1,10-phenanthroline produced [Cp$_2$V(phen)][OTf]$_2$ (**1**) and [Cp$_2$V(bpy)][OTf]$_2$ (**2**), respectively (eq 2). The compounds were characterized by elemental analysis

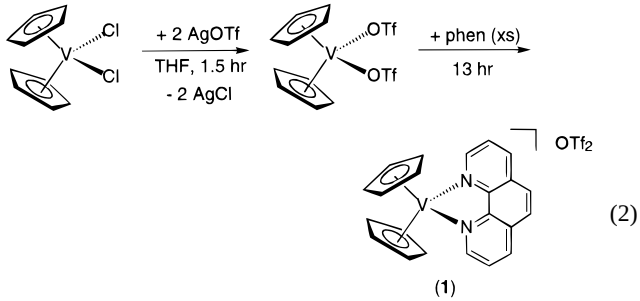

(1) (2)

and MALDI-TOF mass spectrometry. The magnetic moments, as measured by Evans' method, gave $\mu_{eff} = 1.68(12)\ \mu_B$ for **1** and $\mu_{eff} = 1.66(12)\ \mu_B$ for **2**. Both are close to the expected

(41) *SMART Software Reference Manual*, Version 5.0; Bruker Analytical X-ray Instruments Inc., Madison, Wisconsin, 1998.
(42) *SAINT Software Reference Manual*, Version 4.0; Bruker Analytical X-ray Instruments Inc.: Madison, WI, 1996.
(43) *SHELXTL Reference Manual*, Version 5.10; Bruker Analytical X-ray Instruments Inc.: Madison, WI, 1997.
(44) *International Tables for X-ray Crystallography*; Wilson, A. J. C., Ed.; Kluwer Academic Publishers: Dordrecht, 1992; Vol. C, Tables 6.1.1.4 (pp 500−502), 4.2.6.8 (pp 219−222), and 4.2.4.2 (pp 193−197).
(45) Control experiments demonstrated that the small amount of methanol or acetonitrile added did not affect the permeability of the liposome.

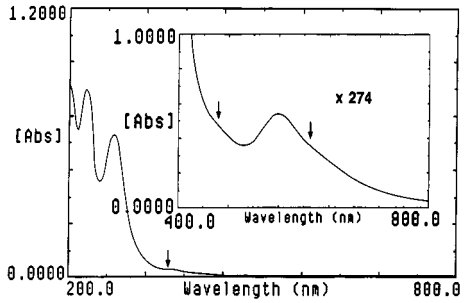

Figure 1. UV−vis spectrum of **1** (2.15×10^{-5} M) in acetonitrile. The inset shows the spectrum in the visible region (5.88×10^{-3} M). The arrows indicate the positions of the weak shoulders.

value for a d^1 system ($\mu_{eff} = 1.72\ \mu_B$). Most chelated complexes of vanadocene(IV) are synthesized via an oxidative pathway with vanadocene(II) and the appropriate organic substrates,[8,9,52−55] but a few have been prepared through the direct substitution of the ancillary positions of the Cp_2V^{IV} ion.[2,3,56,57] Compounds **1** and **2** were prepared using a method similar to that described for the titanium analogues, $[Cp_2Ti(phen)][OTf]_2$ (**3**) and $[Cp_2Ti(bpy)][OTf]_2$ (**4**).[39] Although the reaction to prepare the titanium complexes (**3** and **4**) was instantaneous, the reactions to obtain **1** and **2** required more than 12 h for completion.

UV−Vis and EPR Spectroscopy. The UV−vis absorption spectra of **1** and **2** in acetonitrile have absorption bands at ~17 900 cm^{-1} ($\epsilon = 90-120\ m^{-1}\ cm^{-1}$) along with a shoulder at ~16 600 cm^{-1} (Figure 1). The two weak absorption bands can be assigned to the first two Laporte-forbidden d−d transitions expected from a low-symmetry C_{2v} type molecule. These two transitions are very close in energies, comparable to the well-resolved bands detected for $[Cp_2V(DeDtc)]^+$ (DeDtc = diethyldithiocarbamate), which are at 16 100 and 18 700 cm^{-1}.[22] This feature is different from the Cp_2VCl_2 spectrum, which has a single intense band at 11 800 cm^{-1}, assigned by Stewart et al. on the basis of molecular orbital calculations.[1] A third d−d transition also predicted from the Hückel LCAO calculations is observed for **1** and **2** as a weak shoulder at ~22 400 cm^{-1} ($\epsilon \approx 90\ m^{-1}\ cm^{-1}$).[1,4] There is a significant difference (hypsochromic shift) in the energies of the d−d transitions compared to those of the Cp_2VCl_2 spectral bands. This large blue shift is probably due to the difference in the ligand field effects of the two types of donor ligands.[58,59] The characteristic intense band for a typical Cp ring to V(IV) metal ion charge-transfer transition (LMCT)[1] is also detected at approximately 28 200 cm^{-1} ($\epsilon \approx 2500\ M^{-1}\ cm^{-1}$) for both complexes. This LMCT band is very pronounced for **1** but appears as a shoulder for **2**. In the latter case, the $\pi-\pi^*$ transition of the coordinated bipyridine ligand is shifted about 50 nm more to the low-energy region than that of **1**. This is expected from the higher degree of π−electron delocalization in the expanded planar ring system of phen compared to bpy.[60] This shift is also observed in the UV−vis spectrum of the titanocene(IV) analogues, **3** and **4**.[61]

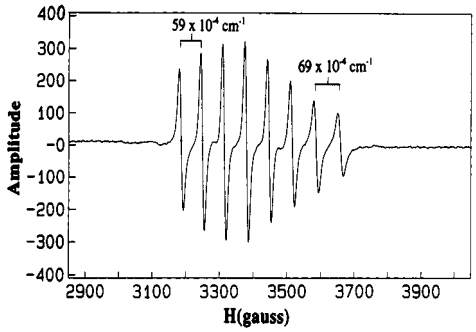

Figure 2. X-band EPR spectrum of 1×10^{-3} M complex **1** in PBS. The experimental conditions and operating frequency are $T = 298$ K, pH= 7.2, $t = 5$ min, $\nu = 9.5597$ GHz, modulation amplitude = 3.984 G at 100 kHz, and receiver gain = 5×10^3.

Table 1. Electrochemical and ESR Data for $[Cp_2V(phen)][OTf]_2$ (**1**) and $[Cp_2V(bpy)][OTf]_2$ (**2**)

electrochemical data		EPR parameters		
$E_{1/2}$ (mV)	solvent	$\langle g \rangle$	$\langle A \rangle$ (cm^{-1})	solvent
		Complex **1**		
−628	acetonitrile[a]	1.98	62.66×10^{-4}	acetonitrile
−1732[b]				
−1978		1.981	62.62×10^{-4}	PBS
−716	PBS[c]			
		Complex **2**		
−616	acetonitrile[a]	1.996	61.06×10^{-4}	acetonitrile
−1714[b]				
−1998		1.999	60.44×10^{-4}	PBS
−717	PBS[c]			

[a] Referenced to $Cp_2Fe^{+/0}$ in acetonitrile. [b] E_{pc} value. [c] Referenced to $Cp_2Fe^{+/0}$ in PBS.

The room-temperature EPR spectra of **1** and **2** in both acetonitrile and PBS solutions show a typical isotropic eight-line resonance in the range $g = 1.98-1.999$ with a ^{51}V ($I = {}^7/_2$) isotropic hyperfine coupling constant $\langle A_{av} \rangle$ of 62.66×10^{-4} and 61.06×10^{-4} cm^{-1}, respectively (Figure 2 and Table 1). Due to second-order perturbation effects,[62] a nonuniform line spacing is observed for both complexes. The $\langle A_{av} \rangle$ values are comparable to those of $Cp_2V(trop)^+$ (trop = 2-hydroxy-2,4,6-cycloheptatrien-1-onate) ($\langle A_{av} \rangle = 61 \times 10^{-4}$ cm^{-1})[56] but are significantly lower than those of Cp_2VX_2 systems, where X= Cl^-, N_3^-, SCN^-, and $SeCN^-$ ($\langle A_{av} \rangle \sim 68 \times 10^{-4}$ cm^{-1})[1] and considerably higher than those of the ethanedithiolato ($\langle A_{av} \rangle = 51 \times 10^{-4}$ cm^{-1}) and mercaptocatecholato ($\langle A_{av} \rangle = 42 \times 10^{-4}$ cm^{-1}) chelated complexes.[8] The observed difference in the anisotropic hyperfine coupling constant for **1** and **2**, compared to the vanadocene(IV) halides or pseudohalides, is due to the $d\pi-p\pi^*$ back-bonding effects of a d^1 system in the presence of

(46) Bramhall, J.; Hofmann, J.; DeGuzman, R.; Montestruque, S.; Schell, R. *Biochemistry* **1987**, *26*, 6330.
(47) Gutteridge, J. M. C.; Quinlan, G. J.; Clark, I.; Halliwell, B. *Biochim. Biophys. Acta* **1985**, *835*, 441.
(48) Quinlan, G. J.; Halliwell, B.; Moorhouse, C. P.; Gutteridge, J. M. C. *Biochim. Biophys. Acta* **1988**, *962*, 196.
(49) Deleers, M.; Servais, J.-P.; Wulfert, E. *Biochim. Biophys. Acta* **1985**, *813*, 195.
(50) Gutteridge, J. M. C. *Anal. Biochem.* **1975**, *69*, 518.
(51) Setaka, M.; Kirino, Y.; Ozawa, T.; Kwan, T. *J. Catal.* **1969**, *15*, 209.
(52) Fochi, G.; Floriani, C. *J. Chem. Soc., Dalton Trans.* **1983**, 1515.
(53) Gambarotta, S.; Fiallo, M. L.; Floriani, C.; Chiesi-Villa, A.; Guastini, C. *Inorg. Chem.* **1984**, *23*, 3532.
(54) Gambarotta, S.; Floriani, C.; Chiesi-Villa, A.; Guastini, C. *Organometallics* **1986**, *5*, 2425.
(55) Muller, E. G.; Watkins, S. F.; Dahl, L. F. *J. Organomet. Chem.* **1976**, *111*, 73.
(56) Doyal, G.; Tobias, R. S. *Inorg. Chem.* **1968**, *7*, 2479.
(57) Doyal, G.; Tobias, R. S. *Inorg. Chem.* **1968**, *7*, 2484.
(58) Lever, A. P. B. *Inorganic Electronic Spectroscopy*; Elsevier: Amsterdam, 1984.
(59) Figgis, B. N. *Introduction to Ligand Fields*; Wiley-Interscience: New York, 1966.
(60) Seddon, E. A.; Seddon, K. R. *The Chemistry of Ruthenium*; Elsevier: Amsterdam, 1984; pp 1193−1214 and references therein.
(61) The UV−vis spectral data are not reported in the literature. UV−vis for **3** (CH_3CN, nm (ϵ)): 406 (2400), 347 (sh, 3000), 272 (45 000), 223 (50 000). UV−vis for **4** (CH_3CN, nm (ϵ)): 383 (sh, 1400), 319 (15 000), 241 (23 000), 215 (32 000).
(62) Rogers, R. N.; Pake, G. E. *J. Chem. Phys.* **1960**, *33*, 1107.

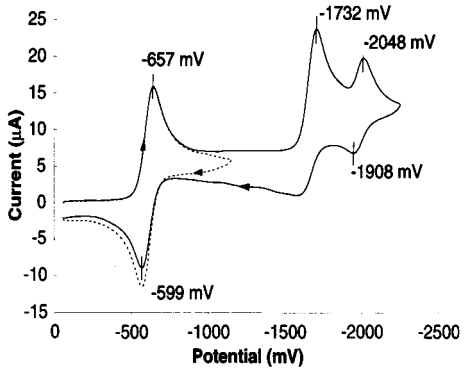

Figure 3. Cyclic voltammograms of **2** in acetonitrile (0.1 M TABP). Scan rate = 200 mV/s. Referenced to $Cp_2Fe^{+/0}$ in acetonitrile solution.

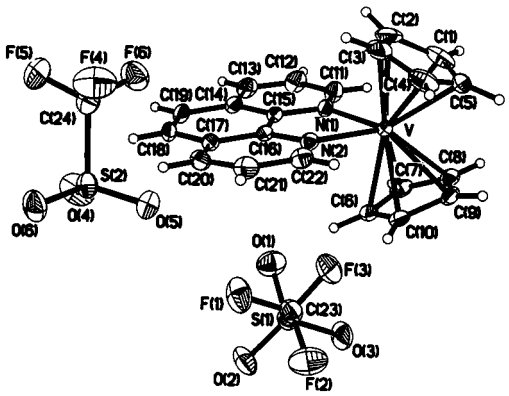

Figure 4. ORTEP drawing of $[Cp_2V(phen)][OTf]_2$ (**1**) with 30% probability anisotropic displacement parameters (room temperature).

coordinated phen or bpy type π-acid ligands.[63] The significant difference in the coupling constant parameter between η^2-iminoacyl or η^2-acetylene vs dihalide or dipseudohalide coordinated complexes cannot be due to the reduced L−V−L angles as suggested by others.[64] In fact, this contradicts the results obtained for **1** and **2** when compared to the sulfur coordinated complexes of vanadocene(IV). The S−V−S angles of the 1,2-benzenedithiolato or 1,3-propanedithiolato complexes are considerably higher than the N−V−N angles for **1** and **2** (vide infra), yet a substantial decrease in the $\langle A_{av} \rangle$ value for the sulfide coordinated species compared to **1** and **2** was seen. These discrepancies may be rationalized from an increased covalent character in the vanadium−sulfur bonding[2,3] over a V−N coordinated bond. This higher covalancy in V−S bonding would provide greater π-electron delocalization compared to the bond caused by the dπ−pπ^* back-bonding of the phen or bpy type π-acceptor ligands in **1** or **2**. Presumably, a similar back-bonding effect also occurs for $Cp_2V(trop)^+$ as the tropolone ligand also has a π-delocalized ring in the vicinity of oxygen donors and could be responsible for the comparable $\langle A_{av} \rangle$ value.

Electrochemistry. Although extensive heterogeneous electron-transfer properties have been documented for Cp_2VCl_2[65−67] and its related analogues,[68] there is very little information available on the chelated vanadocene(IV) complexes.[22,69] Cyclic voltammetric studies of **1** and **2** in acetonitrile show that both complexes undergo identical electron-transfer processes over the potential range +2.1 to −2.5 V (vs the $Cp_2Fe^{+/0}$ couple). As illustrated in Figure 3 and Table 1, each complex displays one reversible couple, centered at −0.62 V, attributable to the $V^{III/IV}$ redox process. This is followed by a $1e^-$ irreversible reduction wave at −1.73 V and another quasireversible redox process with an $E_{1/2}$ of about −2.0 V. The $V^{III/IV}$ couple is significantly more positive (∼400 mV) than those of the corresponding dithiocarbamato complexes ($E_{1/2}$ for $[Cp_2V(DeDtc)]^{0/+} = -1.027$ V vs $Cp_2Fe^{0/+}$ in CH_3CN).[22] This may be due to the destabilization of the e_g orbitals of the degenerate d^1 system in the presence of σ-donor and π-acceptor ligands such as phen or bpy compared to the dithiocarbamate ligand, which is believed to be σ- and π-donor in character.[70,71] The dπ −pπ^* back-bonding effect could make the e_g levels of **1** and **2** more susceptible to the accommodation of an extra electron, whereas the highly stabilized vanadium d orbitals occurring through V−S bonding require higher electrode potential. The third reductive couple located at ∼−1.98 V represents considerably less than a full $1e^-$ process, probably resulting from an electron-transfer-induced chemical reaction (EC mechanism) after the system undergoes a second redox reaction at −1.73 V. It has been noted that, on the cyclic voltammetric time scale, vanadium(III) complexes can release their ligands from the ancillary position after a one- or two-electron reduction.[63,64] The origin of this third redox couple is not the $Cp_2V^{I/II}$ couple, as this is reported to be at −3.3 V,[68] nor is it the reduction of the phen or bpy coordinated ligands.[72−74] It may be a metal-centered reduction from an unknown vanadium(II) complex. To our surprise, unlike Cp_2VCl_2 or $Cp_2V(acac)^+$ (acac = acetyl acetonate),[75] there is no detectable $V^{IV/V}$ couple observed in the available solvent window in acetonitrile (0.0 to +2.2 V). The extra stabilization of the d^1 electron through back-bonding effects could impart such results. The complete electrode stoichiometry is represented by eq 3.

$$[Cp_2V^{IV}(phen)]^{2+} \underset{-e^-}{\overset{+e^-}{\rightleftharpoons}} [Cp_2V^{III}(phen)]^{+} \underset{-e^-}{\overset{+e^-}{\rightleftharpoons}} [Cp_2V^{II}(phen)] \longrightarrow$$

$$\text{unknown products} \underset{-e^-}{\overset{+e^-}{\rightleftharpoons}} \text{unknown reduction products} \quad (3)$$

In physiological buffer, these two complexes display only one $V^{III/IV}$ reversible redox couple centered at ∼−0.72 V over a potential range of −0.9 to +0.9 V, indicating no alteration of the stereochemistry around the metal center on the cyclic voltammetric time scale upon reduction. Both the V(IV) complexes show fair stability in aqueous solution. The peak current height, (I_p) of the $V^{III/IV}$ couple was reduced approximately 15% after 3 days of standing at room temperature. Similar results were also observed by EPR spectroscopy.

Structural Studies. ORTEP diagrams of **1** and **2** are depicted in Figures 4 and 5, respectively, along with the atom-numbering scheme. The crystallographic data are presented in Table 2, and selected bond distances and angles are given in Table 3. The

(63) Taube, H. *Pure Appl. Chem.* **1979**, *51*, 901.
(64) Petersen, J. L.; Griffith, L. *Inorg. Chem.* **1980**, *19*, 1852.
(65) Holloway, J. D. L.; Geiger, W. E. *J. Am. Chem. Soc.* **1979**, *101*, 2038.
(66) Mugnier, Y.; Moise, C.; Laviron, E. *New J. Chem.* **1982**, *6*, 197.
(67) Kuzharenko, S. V.; Strelets, V. V. *Izv. Akad. Nauk SSSR, Ser. Khim.* **1987**, 297.
(68) Dorer, B.; Diebold, J.; Weyand, O.; Brintzinger, H.-H. *J. Organomet. Chem.* **1992**, *427*, 245.
(69) Bond, A. M.; Casey, A. T.; Thackeray, J. R. *Inorg. Chem.* **1973**, *4*, 887.
(70) Coucouvanis, D. *Prog. Inorg. Chem.* **1970**, *11*, 233−371.
(71) Steggerda, J. J.; Cras, J. A.; Willemse, J. *Recl. Trav. Chim. Pays-Bas* **1981**, *100* (2), 41.
(72) Saji, T.; Aoyagui, S. *J. Electroanal. Chem. Interfacial Electrochem.* **1975**, *60*, 1.
(73) Guadualupe, A. R.; Usifer, D. A.; Potts, K. T.; Hurrell, H. C.; Mogstad, A.-E.; Abruna, H. D. *J. Am. Chem. Soc.* **1988**, *110*, 3462.
(74) Saji, T.; Aoyagui, S. *J. Electroanal. Chem. Interfacial Electrochem.* **1975**, *63*, 31.
(75) Ghosh, P.; Uckun, F. M. Unpublished data.

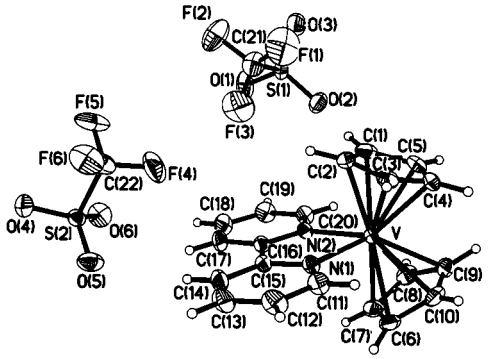

Figure 5. ORTEP drawing of $[Cp_2V(bpy)][OTf]_2$ (**2**) with 30% probability anisotropic displacement parameters (room temperature).

Table 2. Crystallographic Data for $[Cp_2V(phen)][OTf]_2$ (**1**) and $[Cp_2V(bpy)][OTf]_2$ (**2**)

complex	**1**	**2**
empirical formula	$C_{24}H_{18}F_6N_2O_6S_2V$	$C_{22}H_{18}F_6N_2O_6S_2V$
fw	659.46	635.44
crystal system	monoclinic	monoclinic
space group	$P2_1/n$	$P2_1/c$
a (Å)	10.2763(5)	10.6451(6)
b (Å)	18.1646(9)	18.3863(10)
c (Å)	13.5741(7)	12.6993(7)
β (deg)	99.4150(10)	98.6220(10)
λ (Å)	0.710 73	0.710 73
V (Å^3)	2499.7(2)	2457.5(2)
Z	4	4
d (calcd) (g/cm^3)	1.752	1.718
abs coeff (mm^{-1})	0.655	0.663
F(000)	1332	1284
crystal size (mm)	0.50 × 0.30 × 0.10	0.40 × 0.20 × 0.20
T (K)	293(2)	293(2)
θ range (deg)	1.89−28.28	1.93−28.30
limiting indices	$-12 < h < 13$	$-14 < h < 9$
	$-22 < k < 23$	$-24 < k < 24$
	$-17 < l < 17$	$-16 < l < 16$
no. of reflns collected	15 058	14 839
no. of independ reflns	5723	5626
no. of restraints	0	0
no. of params	371	353
final R, R_w [$I > 2\sigma(I)$]	4.00%, 9.65%	4.60%, 10.06%
goodness-of-fit on F^2	1.042	1.085

two π-bonded Cp rings and the two nitrogen atoms of phenanthroline (**1**) or bipyridine (**2**) formally occupy the pseudotetrahedral coordination sites around the vanadium(IV) center. The cyclopentadienyl ring A (C1−C5) and ring B(C6−C10) are planar in both complexes. The dihedral angle between the two cyclopentadienyl rings is 46.07° for **1** and 46.17° for **2**. The bisecting angles defined by the VN_2 plane with respect to the two Cp rings are 26.97(6)° (ring A) and 19.10(7)° (ring B) for **1** and 21.24(6)°(ring A) and 24.93(13)° (ring B) for **2**. The chelated ring is inclined closer to one of its neighboring Cp rings, and it is not clear to us at present why the heterocyclic chelated ring is shifted toward one of the Cp rings over the other. The degree of inclination between the VN_2 plane with respect to the plane of the remaining carbon atoms is more pronounced for phen (3.89(5)°) than for bpy (1.69(11)°). This could be attributed to the difference between the heterocyclic ligands themselves. A similar effect is also observed for titanium analogues.[39] The vanadium atom projects 1.96 Å below the center of ring A and 1.96 Å above the mean plane of ring B for the complexes. The angles between the ring centroid−V−ring centroid vectors for **1** and **2** are 133.63 and 133.24°, respectively, which are slightly lower than that in $Cp_2V(DeDtc)^+$ (134.6°)[22] but comparable to those of the titanocene(IV) analogues **3** and **4** (Table 4). This could reflect the higher steric demands of the five-membered chelated phen or bpy unit compared to the four-membered DeDtc ligand. The N1−V−N2 angles are 76.66(8) and 75.69 (8)° in **1** and **2**, respectively. These values are comparable to those of the reported five-membered chelated oxametalacycles of Cp_2V^{IV},[54] as well as to the titanocene(IV) analogues (Table 4), but are significantly smaller when compared with that of the Cp_2V(1,2-benzenedithiolate), complex where the bite angle of the five-membered ring is 79.9°.[9] The relatively larger S−V−S angle compared to the N−V−N angle is probably due to the greater flexibility offered by the thiolate chelated ring vs the rigid phen or bpy ligand where the donor nitrogen centers are fixed in a six-membered heterocycle. The V−N distances are 2.135(1) and 2.129(1) Å for **1** and **2**, which are slightly shorter than the Ti−N bond distances reported for **3** and **4** (Table 4). There is no literature precedent for a single-bonded V−N distance coordinated to a Cp_2V^{IV} unit except for η^2-iminoacyl coordinated vanadocene(IV).[76,77] Crystal structure data revealed that, with the three-membered chelation, the V−N distance is 2.054(4) Å, which is significantly shorter than those observed for **1** and **2**. In the three cases, ligand moieties have the vacant π^* orbital available for back-bonding and the difference in bond lengths could be rationalized in terms of their differences in dπ−pπ***** back-bonding, which is more pronounced for the three-membered η^2-chelated ring. This is supported by the comparison of the V−N (2.054(4) Å) bond distance of the η^2-iminoacyl coordinated complex to that of its d^0 Ti(IV) analogue (2.149(4) Å).[78] Without the involvement of a single d^1 electron in bonding, the M−N distances in such systems would be expected to be very close to each other. This is indeed the case for the titanium compounds when their Ti−N distances are compared with those of the η^2-iminoacyl vs bpy coordinated complexes (**3**).[39,78] The small observed difference between vanadium− (**1** or **2**) or titanium− (**3** or **4**) nitrogen bond distances arises from a delocalization imparted by a d^1 electron via dπ−pπ^* back-bonding.

Table 3. Selected Bond Lengths (Å) and Angles (deg) for $[Cp_2V(phen)][OTf]_2$ (**1**) and $[Cp_2V(bpy)][OTf]_2$ (**2**)

1		**2**	
V−N(1)	2.1344(18)	V−N(1)	2.129(2)
V−N(2)	2.1386(19)	V−N(2)	2.128(2)
V−Cp(A)	1.96	V−Cp(A)	1.96
V−C(1)	2.268(3)	V−C(1)	2.299(3)
V−C(2)	2.297(3)	V−C(2)	2.266(3)
V−C(3)	2.297(3)	V−C(3)	2.283(3)
V−C(4)	2.262(3)	V−C(4)	2.302(3)
V−C(5)	2.277(2)	V−C(5)	2.304(3)
V−Cp(B)	1.96	V−Cp(B)	1.96
V−C(6)	2.263(2)	V−C(6)	2.315(3)
V−C(7)	2.298(2)	V−C(7)	2.293(3)
V−C(8)	2.313(2)	V−C(8)	2.280(3)
V−C(9)	2.310(2)	V−C(9)	2.298(3)
V−C(10)	2.285(2)	V−C(10)	2.294(3)
N(1)−V−N(2)	76.66(7)	N(1)−V−N(2)	75.69(8)
Cp(A)−V−Cp(B)	133.63	Cp(A)−V−Cp(B)	133.24
Cp(A)−V−N(1)	109.06	Cp(A)−V−N(1)	107.92
Cp(A)−V−N(2)	106.90	Cp(A)−V−N(2)	108.56
Cp(B)−V−N(1)	108.11	Cp(B)−V−N(1)	108.04
Cp(B)−V−N(2)	108.15	Cp(B)−V−N(2)	108.53

Membrane Interaction Studies. The concentration dependence for metal-complex-induced permeability of liposomes, as measured by the release of 5(6)-carboxyfluorescein, is shown

(76) Carrier, A. M.; Davidson, J. G.; Barefield, E. K.; Van Derveer, D. G. *Organometallics* **1987**, *6*, 454.
(77) Rettig, M. F.; Wing, R. M. *Inorg. Chem.* **1969**, *8*, 2685.
(78) Van Bolhuis, F.; De Boer, E. J. M.; Teiben, J. H. *J. Organomet. Chem.* **1979**, *170*, 299.

Table 4. Comparison of Selected Bond Lengths and Angles for Compounds **1**−**4**

	bond lengths (Å)				bond angles (deg)		
complex	M−Cp(A)	M−Cp(B)	M−N(1)	M−N(2)	Cp(A)−V−Cp(B)	N(1)−V−N(2)	ref
1	1.96	1.96	2.1351(18)	2.1388(18)	133.63	76.66(7)	this work
2	1.96	1.96	2.129(2)	2.128(2)	133.24	75.69(8)	this work
3	2.019	2.023	2.162(3)	2.168(3)	133.7	76.8(1)	10
4	2.01	2.06	2.14(1)	2.14(1)	133.2	75.7(3)	10

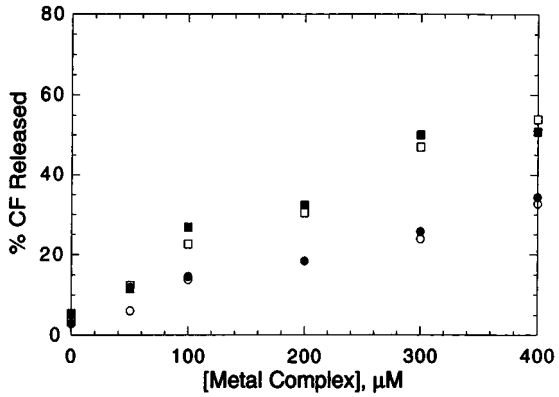

Figure 6. Relative amount of released carboxyfluorescein (CF) after 6 min from CF-loaded PC liposomes as a function of the concentration of added vanadium- or titanium-chelated complexes: (■) **1**; (●) **2**; (□) **3**, (○) **4**.

in Figure 6 for zwitterionic (PC) liposomes. The metal complexes themselves do not interfere with the fluorescence of the carboxyfluorescein probe. At a concentration of 400 μM, the phenanthroline chelated complexes **1** and **3** induce releases of 51% and 54%, respectively, of the entrapped carboxyfluorescein, while the bipyridine chelated complexes **2** and **4** release 34% and 33%, respectively, of the entrapped carboxyfluorescein. Control experiments with all of the chelating ligands confirmed that the free ligands had no effect on the permeation. Furthermore, the membrane permeability effects of the metallocene complexes are not associated with any aggregation of liposomes indicative of membrane disruption, as shown by the lack of an increase in turbidity with addition of any of the metallocene complexes at concentrations up to a 400 μM (data available as Supporting Information).

Current models of the binding of metal coordinated complexes to micelles include the metal center being located near the charged surface to maximize ionic interactions and the hydrophobic ligands buried in the hydrocarbon region to provide favorable interactions with the hydrocarbon chains. This leaves the remaining ligands solvent-accessible in the Gouy−Chapman layer.[79] Increasing the hydrophobicity of the ligands has been shown to increase the depth of binding of the metal coordinated complex.[33] EPR experiments conducted by Turro's group have demonstrated that there is both a lower activation energy and a lower correlation time for motion for $Ru(bpy)_2(phen)$ as compared to $Ru(phen)_3$.[26] The results were rationalized by the hydrophobicity of the phenanthroline ligand leading to a stronger interaction with the hydrophobic micellar core. Recently, DeGraff's group has shown that $Ru(phen)_3$ binds more strongly to zwitterionic and anionic vesicles than $Ru(bpy)_3$ by a factor of almost 10.[30] In our case, the complexes with the phenanthroline ligands should also bind more strongly and be embedded more deeply in the liposomal membrane than the complexes with bipyridine ligands.

(79) Cvec, G.; Marsh, D. *Phospholipid Bilayers*; John Wiley & Sons: New York, 1987; pp 99−129.

Scheme 1. Representation of a Metallocene Complex in a Liposomal Membrane

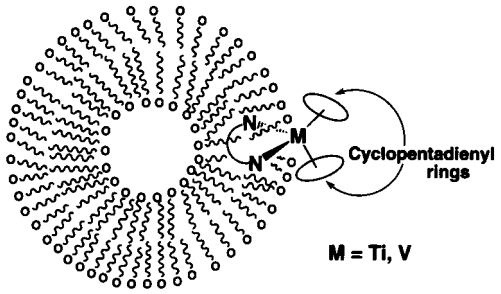

Recently, we described a series of vanadocene-chelated complexes where the permeation of a fluorescent probe out of a liposome was induced by the addition of some vanadocene derivatives.[38] The magnitude of the effect was thought to be modulated by the degree of hydrophobicity and planarity of the ancillary ligand of the complex since there was no correlation between permeation and the charge on the vanadocene derivative or its ability to initiate lipid peroxidation. Changing the ligand from bipyridine (complexes **2** and **4**) to phenanthroline (complexes **1** and **3**) increases the hydrophobicity and rigidity of the molecule, and the result is an increase in the permeability of the liposomal membranes from approximately 35% to approximately 50%, regardless of the cenral metal ion (Figure 6). X-ray data reveal that the structural features are nearly identical in both the vanadocene complexes (**1** and **2**) and their titanium analogues (**3** and **4**) in terms of bond lengths and conformational geometry (Table 4). This confirms that the observed trend is due to the structural details of the complexes. Most likely, the metal complexes are wedged in localized patches of the membrane, rendering it temporarily leaky without affecting the overall integrity of the liposome, as depicted in Scheme 1. The better binding of the phenanthroline complex, as well as its greater size and rigidity, as compared to the bipyridine coordinated complex, could be creating larger areas of leaky patches and hence causing a greater percentage of the dye molecule to leak out.

Because increased membrane permeability is often seen with peroxidation of the membrane lipids in biological systems, they have been thought to be related.[80−82] However, several studies attempting to correlate permeability and lipid peroxidation induced by metal ions, ascorbic acid, glutathione, or γ radiation have proven inconclusive.[83−86] The amount of lipid peroxidation caused by the incubation of PC liposomes with the metal complexes is shown in Figure 7. The vanadocene complexes **1** and **2** induce lipid peroxidation, as measured by the production

(80) Fong, K.-L.; McCay, P. B.; Poyer, J. L.; Keele, B. B.; Misra, H. *J. Biol. Chem.* **1973**, *248*, 7793.
(81) Wills, E. D.; Wilkinson, A. E. *Biochem. J.* **1966**, *99*, 657.
(82) Robinson, J. D. *Arch. Biochem. Biophys*. **1965**, *112*, 170.
(83) Hicks, M.; Bebicki, J. M. *Biochem. Biophys. Res. Commun.* **1978**, *80*, 704.
(84) Nakazawa, T.; Nagatsuka, S. *Int. J. Radiat. Biol*. **1980**, *38*, 537.
(85) Smolen, J. E.; Shohet, S. B. *J. Lipid. Res*. **1974**, *15*, 273.
(86) Leibowitz, M. E.; Johnson, M. C. *J. Lipid. Res*. **1971**, *12*, 662.

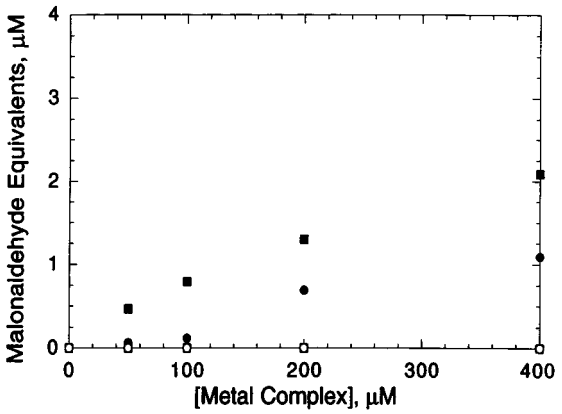

Figure 7. Effects of vanadium and titanium complexes on lipid peroxidation. PC liposomes were incubated in the presence of vanadium- or titanium-chelated complexes: (■) **1**; (●) **2**; (□) **3**; (○) **4**. Lipid peroxidation was evaluated as the production of 2-thiobarbituric acid reactive substances and is reported in malonaldehyde equivalents.

of 2-thiobarbituric acid reactive substances. The titanium complexes **3** and **4**, on the other hand, do not initiate any peroxidation of the lipids. The mechanism of initiation of lipid peroxidation by vanadocene chelated complexes is not known. Lipid peroxidation is thought to occur through a free radical chain mechanism whereby an initial free radical, most likely a hydroxyl or superoxide radical, attacks the allylic hydrogens of the unsaturated lipids.[87] Hydroxyl radicals can be formed by some but not all vanadocene complexes in a Fenton-type reaction with the conversion of V(IV) to V(V).[88] In the case of **1** and **2**, the addition of excess hydrogen peroxide to a PBS solution containing **1** or **2** and a spin trap reagent failed to detect any spin trap−hydroxyl radical products by EPR spectroscopy (data available as Supporting Information). The fact that **1** and **2** initiate the peroxidation of the lipids without forming hydroxyl radicals puts them in the category of the other vanadocene derivatives which inititate lipid peroxidation by a different and as yet unknown mechanism, currently under investigation. Titanium(IV), however, is incapable of initiating this process presumably because these species are unable to undergo further metal-centered oxidation. The phenanthroline vanadocene derivative **1** causes more peroxidation of the lipids than the bipyridine vanadocene derivative **2**. The reason for the differing degrees of peroxidation is not known. It may be related to the propensity of the vanadocene complex to go from V(IV) to V(V), but we are unable to measure the potential difference between the two complexes in the available solvent window. It may also be related to the degree of binding of the vanadocene complex to the liposome, which could lead to greater exposure of the vanadocene complex to the double bonds in the hydrocarbon chains or to a combination of both potential difference and binding. In any case, it is clear that the ability of metallocene-chelated complexes to alter the permeability of liposomal membranes is related to their structural configuration rather than their capacity to initiate lipid peroxidation.

(87) Konigs, A. W. T. In *Liposome Technology*; Gregoriadis, G., Ed.; CRC: Boca Raton, FL, 1992; Vol. 1, pp 139−161 and references therein.

(88) Ghosh, P.; D'Cruz, O. J.; DuMez, D. D.; Peitersen, J.; Uckun. F. M. *J. Inorg. Biochem.*, in press.

Concluding Remarks

In summary, the first 1,10-phenanthroline- and 2,2′-bipyridine-chelated vanadocene(IV) complexes have been synthesized and characterized by cyclic voltammetry, EPR and UV−vis spectroscopy, and X-ray crystallography. It was apparent from the characterization that there was significant involvement of the d^1 electron of vanadocene(IV) in $d\pi-p\pi^*$ back-bonding with the π-acid ligands.

The abilities of these vanadocene-chelated complexes and their titanium analogues to cause leakage of a fluorescent probe through liposomal membranes were compared. The results indicated that this property is related to the overall structural features of the complexes and not to the central metal ion itself. A combination of the size and rigidity of the structures and the hydrophobicity of the chelated ligands probably plays the most important role in this phenomenon.

The vanadocene complexes, **1** and **2**, unlike their titanium analogues, **3** and **4**, initiated lipid peroxidation. EPR spin-trapping experiments revealed that lipid peroxidation by **1** or **2** is not initiated by the conventionally proposed hydroxyl radical pathway. Additionally, we did not observe any correlation between the induction of permeability of the unilamellar liposomes and the amount of lipid peroxidation produced by these metal complexes.

Acknowledgment. We thank Steve Philson at the Department of Chemistry, University of Minnesota, for his assistance with the EPR spectroscopy.

Supporting Information Available: Listings of structure refinement details, anisotropic displacement parameters for non-hydrogen atoms, coordinates of hydrogen atoms and their isotropic displacement parameters, all bond lengths and angles, and torsional angles for $[Cp_2V(phen)][OTf]_2$ (**1**) and $[Cp_2V(bpy)][OTf]_2$ (**2**), a figure depicting the vanadocene-chelated complex concentration dependent aggregation with PC liposomes, and figures for EPR spin-trapping experiments. This material is available free of charge via the Internet at http://pubs.acs.org.

IC9902469